

# A NURBS-based Discontinuous Galerkin Framework for Compressible Aerodynamics

Stefano Pezzano, Régis Duvigneau

Université Côte d'Azur, Inria, CNRS, LJAD  
e-mail: stefano.pezzano@inria.fr, regis.duvigneau@inria.fr

AIAA Aviation Forum, 15-19 June 2020

*Copyright © by Stefano Pezzano and Régis Duvigneau. Published by the American Institute of Aeronautics and Astronautics, Inc., with permission.*

# Outline

- 1 **Introduction to IsoGeometric Analysis**
- 2 **NURBS-Based Discontinuous Galerkin**
- 3 **Extension to deformable domains**
- 4 **ALE-AMR coupling**

# Outline

1 **Introduction to IsoGeometric Analysis**

2 NURBS-Based Discontinuous Galerkin

3 Extension to deformable domains

4 ALE-AMR coupling

# The IsoGeometric paradigm

- Industrial drawing is done using CAD software
- Meshes for numerical simulation are generated from CAD data
- Classical finite elements adopt a different geometric representation with respect to CAD
- Conversion between the two formats is **time consuming** and the process is not completely **automatic**
- **IsoGeometric Analysis**: CAD basis functions (NURBS) are employed as approximation space for finite elements

# Bernstein polynomials

The building blocks of the CAD representation are the Bernstein polynomials:

$$B_i^p(\xi) = \binom{p}{i} \xi^i (1 - \xi)^{p-i} \quad \xi \in [0, 1]$$

Some important properties:

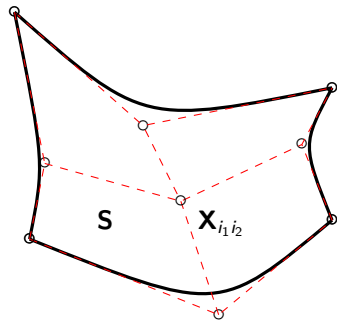
- non-negativity:  $B(\xi) \geq 0, \forall \xi$
- partition of unity:  $\sum_i B_i^p(\xi) = 1, \forall \xi$
- $B_0^p(0) = B_p^p(1) = 1$
- they can be computed recursively

# Bézier surfaces

Parametric polynomial surfaces defined as:

$$\mathbf{S}(\xi, \eta) = \sum_{i_1=1}^{p+1} \sum_{i_2=1}^{p+1} B_{i_1}^p(\xi) B_{i_2}^p(\eta) \mathbf{X}_{i_1 i_2}$$

The coefficients  $\mathbf{X}_{i_1 i_2}$  are called **control points**.



Conics are not **exactly** represented with polynomials, **rational** Bézier surfaces are therefore introduced:

$$R_{i_1 i_2}^p(\xi, \eta) = \frac{B_{i_1}^p(\xi) B_{i_2}^p(\eta) \omega_{i_1 i_2}}{\sum_{j_1=1}^{p+1} \sum_{j_2=1}^{p+1} B_{j_1}^p(\xi) B_{j_2}^p(\eta) \omega_{j_1 j_2}} \quad \mathbf{S}(\xi, \eta) = \sum_{i_1=1}^{p+1} \sum_{i_2=1}^{p+1} R_{i_1 i_2}^p(\xi, \eta) \mathbf{X}_{i_1 i_2}$$

The coefficients  $\omega_{i_1 i_2}$  are called **weights**.

# B-Splines and NURBS

- complex geometries require high-degree functions when using a single polynomial patch
- B-Spline functions  $N_i^p(\xi)$  are the piecewise extension of Bernstein polynomials
- Parametric domain  $\hat{\Omega} = [\xi_1, \xi_l]$ , discretized by the knot vector  $\Xi = (\xi_1, \dots, \xi_i, \dots, \xi_l)$
- Recursive evaluation:

$$N_i^0(\xi) = \begin{cases} 1 & \text{if } \xi_i \leq \xi < \xi_{i+1} \\ 0 & \text{otherwise} \end{cases}$$

$$N_i^p(\xi) = \frac{\xi - \xi_i}{\xi_{i+p} - \xi_i} N_i^{p-1}(\xi) + \frac{\xi_{i+p+1} - \xi}{\xi_{i+p+1} - \xi_{i+1}} N_{i+1}^{p-1}(\xi)$$

- NURBS are the rational extension of B-Splines:

$$R_{i_1 i_2}^p(\xi, \eta) = \frac{N_{i_1}^p(\xi) N_{i_2}^p(\eta) \omega_{i_1 i_2}}{\sum_{j_1=1}^{n_1} \sum_{j_2=1}^{n_2} N_{j_1}^p(\xi) N_{j_2}^p(\eta) \omega_{j_1 j_2}}$$

# Outline

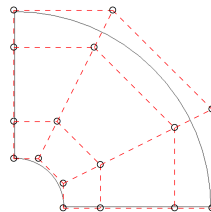
- 1 Introduction to IsoGeometric Analysis
- 2 NURBS-Based Discontinuous Galerkin**
- 3 Extension to deformable domains
- 4 ALE-AMR coupling



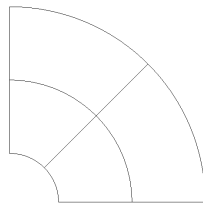
# Bézier Extraction

- NURBS suitable for CG (classic IgA)
- Rational Bézier functions are DG-compliant
- Bézier patches can be **extracted** from NURBS
- Extraction based on multiple **knot refinements**
- Geometry is **unaltered**

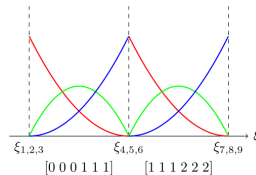
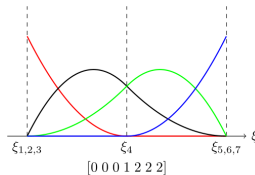
**CAD geometry now compatible with DG discretization!**



NURBS patch  
(4 × 4, degree 2)



Four disconnected  
rational Bézier patches



# DG formulation

- Navier-Stokes equations in divergence form:

$$\frac{\partial \mathbf{W}}{\partial t} + \nabla \cdot \mathbf{F} = 0$$

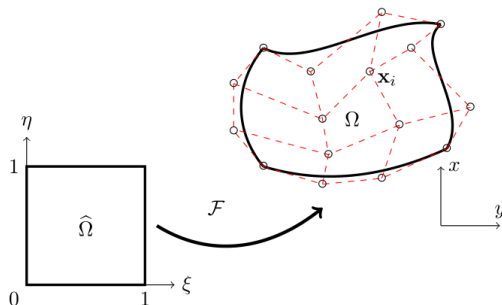
- Each element is a **rational Bézier patch**:

$$\begin{pmatrix} \mathbf{x} \\ \mathbf{w}_h \end{pmatrix} = \sum_{i=1}^{(p+1)^2} R_i(\xi, \eta) \begin{pmatrix} \mathbf{x}_i \\ \mathbf{w}_i \end{pmatrix}$$

- The **weak formulation** is:

$$\frac{d\mathbf{w}_i}{dt} \int_{\hat{\Omega}_j} R_k R_i |J_{\Omega}| d\hat{\Omega} = \int_{\hat{\Omega}_j} \nabla R_k \cdot \mathbf{F} |J_{\Omega}| d\hat{\Omega} - \oint_{\partial \hat{\Omega}_j} R_k \mathbf{F}^* |J_{\Gamma}| d\hat{\Gamma}$$

- Integrals computed in the **parametric domain**,  $J_{\Omega}$  and  $J_{\Gamma}$  are **metric terms**



# DG formulation, cont'd

- Elements coupled through numerical flux  $\mathbf{F}^*$
- $\mathbf{F}^* = \mathbf{F}^*(\mathbf{w}_h^+, \mathbf{w}_h^-, \mathbf{n})$  is a consistent Riemann solver:

$$\mathbf{F}^*(\mathbf{w}_0, \mathbf{w}_0, \mathbf{n}) = \mathbf{F}(\mathbf{w}_0) \cdot \mathbf{n}$$

- Space integrals computed through Gauss quadrature
- Time evolution of DOFs described by system of ODEs:

$$\mathcal{M} \frac{d\mathbf{w}}{dt} = \mathcal{R}(\mathbf{w}_h)$$

- Explicit Runge-Kutta (RK4 or RK3 SSP) method for time integration

## 2D Laminar Cylinder

- **Exact** cylinder representation, using **rational** functions
- Polynomial degree: 3, 4, 5
- 3 refinement levels: 1065, 2145 and 4455 elements
- $M_\infty = 0.2$ ,  $Re = 500$

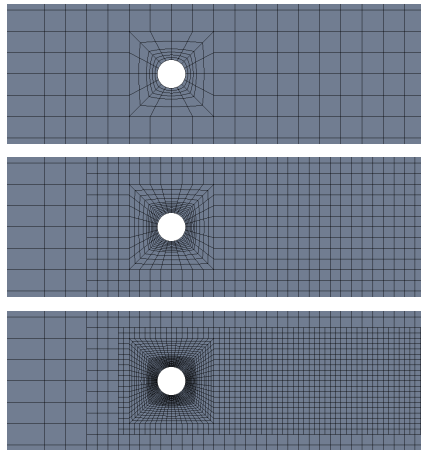
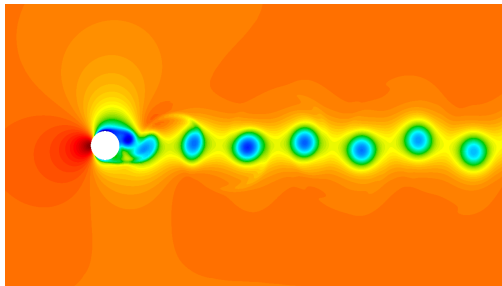
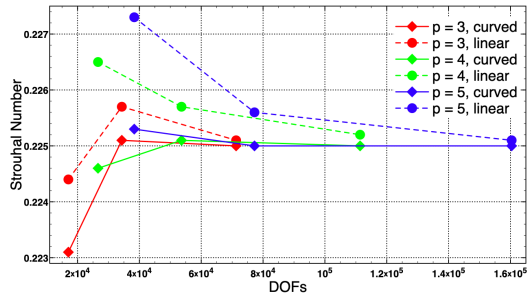
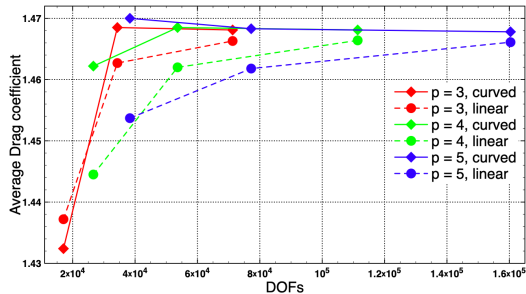
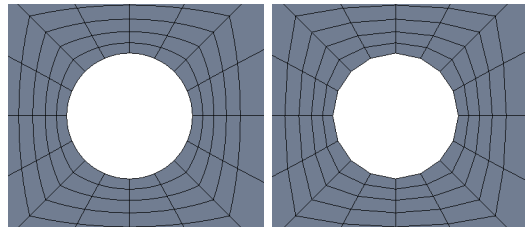


Figure: mesh levels

# Mesh convergence

- Comparison with linear grid
- Faster convergence with degree 4 and 5, **with curved boundary**
- **Lower convergence rate with linear geometry**



# Outline

- 1 Introduction to IsoGeometric Analysis
- 2 NURBS-Based Discontinuous Galerkin
- 3 Extension to deformable domains**
- 4 ALE-AMR coupling

# ALE scheme

- The formulation proposed by Nguyen<sup>1</sup> is extended to Bézier elements:

$$\frac{d}{dt} \left( \mathbf{w}_i \int_{\hat{\Omega}_j} R_k R_i |J_{\Omega}| d\hat{\Omega} \right) = \int_{\hat{\Omega}_j} \nabla R_k \cdot (\mathbf{F} - \mathbf{V}_g \mathbf{w}_h) |J_{\Omega}| d\hat{\Omega} - \oint_{\partial \hat{\Omega}_j} R_k \mathbf{F}_{ale}^* |J_{\Gamma}| d\hat{\Gamma}$$

- Consistency condition** for  $\mathbf{F}_{ale}^* = \mathbf{F}_{ale}^*(w_h^+, w_h^-, \mathbf{V}_g, \mathbf{n})$  becomes:

$$\mathbf{F}_{ale}^*(\mathbf{w}_0, \mathbf{w}_0, \mathbf{V}_g, \mathbf{n}) = \mathbf{F}(\mathbf{w}_0) \cdot \mathbf{n} - (\mathbf{V}_g \cdot \mathbf{n}) \mathbf{w}_0$$

- Constant solutions not exactly preserved due to metric terms
- Mass matrix is time dependent:

$$\frac{d}{dt} (\mathcal{M} \mathbf{w}) = \mathcal{R}(\mathbf{w}_h, \mathbf{V}_g)$$

<sup>1</sup>V. T. Nguyen, *An arbitrary Lagrangian-Eulerian discontinuous Galerkin method for simulations of flows over variable geometries*, Journal of Fluids and Structures 26 (2010), 312-329

# NURBS-based mesh movement

- **Isoparametric** paradigm used to define grid velocity field:

$$\begin{pmatrix} \mathbf{x} \\ \mathbf{v}_g \\ \mathbf{w}_h \end{pmatrix} = \sum_{i=1}^{(p+1)^2} R_i(\xi, \eta) \begin{pmatrix} \mathbf{x}_i \\ \mathbf{v}_{g,i} \\ \mathbf{w}_i \end{pmatrix}$$

- Time evolution of control point net:

$$\frac{d\mathbf{x}_i}{dt} = \mathbf{v}_{g,i}$$

- **Arbitrarily high-order deformations**
- Explicit movement: distribution of  $\mathbf{v}_{g,i}$  is imposed at each time step
- Integration with RK4 or RK3 SSP



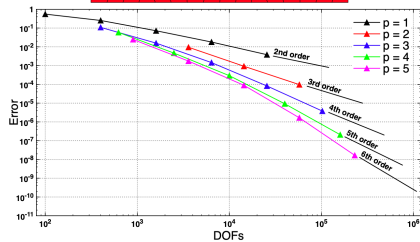
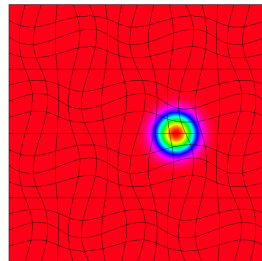
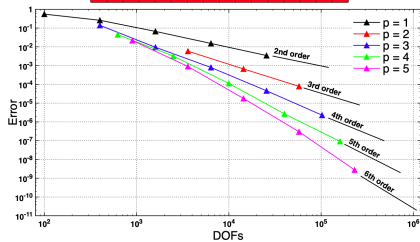
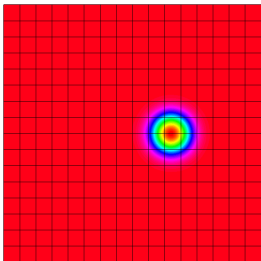
# Isentropic vortex test case

- Euler equations
- Advection of an isentropic vortex:

$$\begin{cases} \rho = \left( 1 - \frac{\gamma-1}{16\gamma\pi^2} \beta^2 e^{2(1-r^2)} \right)^{\frac{1}{\gamma-1}} \\ u = 1 - \beta e^{1-r^2} \frac{y-y_0}{2\pi} \\ v = \beta e^{1-r^2} \frac{x-t-x_0}{2\pi} \\ p = \rho^\gamma \end{cases}$$

- Two configurations are compared:
  - fixed mesh
  - deforming mesh:  $u_g(\mathbf{x}, t) = v_g(\mathbf{x}, t) = \sin\left(\frac{\pi}{2}x\right) \sin\left(\frac{\pi}{2}y\right) \sin(2\pi t)$

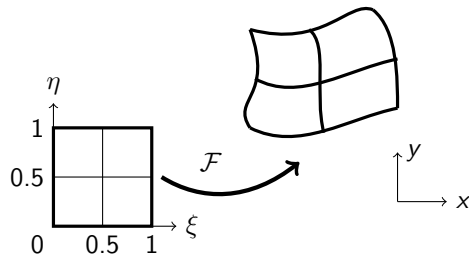
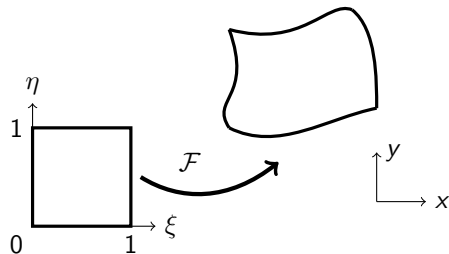
# Error analysis



# Outline

- 1 Introduction to IsoGeometric Analysis
- 2 NURBS-Based Discontinuous Galerkin
- 3 Extension to deformable domains
- 4 ALE-AMR coupling**

# Adaptive Mesh Refinement

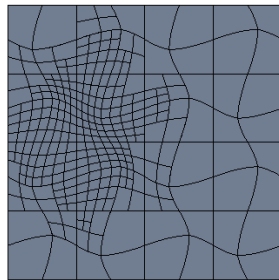
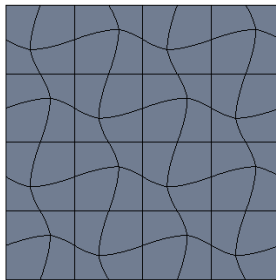
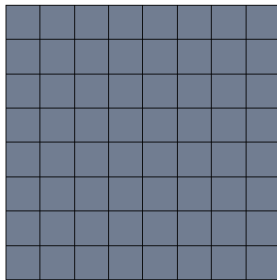


- Isotropic quadtree-like refinement
- Element and solution splitting based on **knot insertion**
- Very coarse, but **CAD-consistent**, initial meshes
- Error indicator based on interface jumps:

$$\varepsilon_j = \sum_{k \in \mathcal{N}_j} \int_{\Gamma_{jk}} \| \mathbf{w}|^j - \mathbf{w}|^k \| \, d\Gamma$$

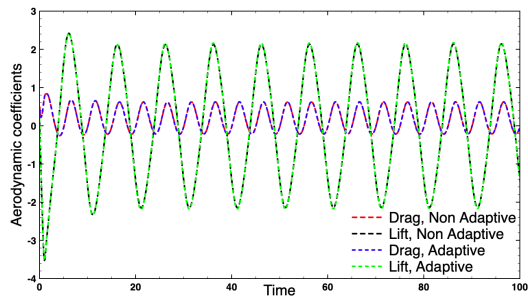
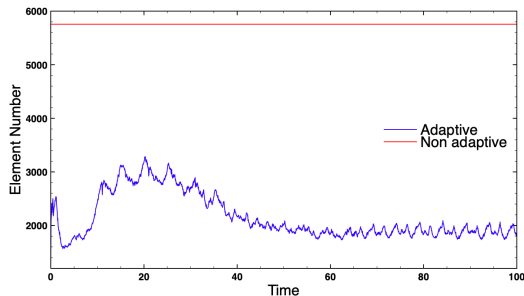
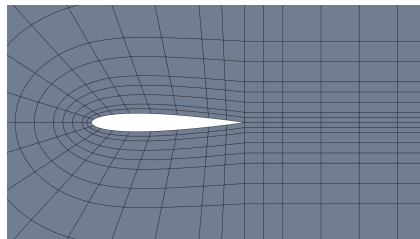
# Coupling with mesh movement

- Moving and deforming bodies = **unsteady flows**
- Non-linear deformations can make refinement irreversible
- Mesh movement must be AMR-compatible
- Mesh velocity is computed on Level-0 grid and propagated via knot insertion

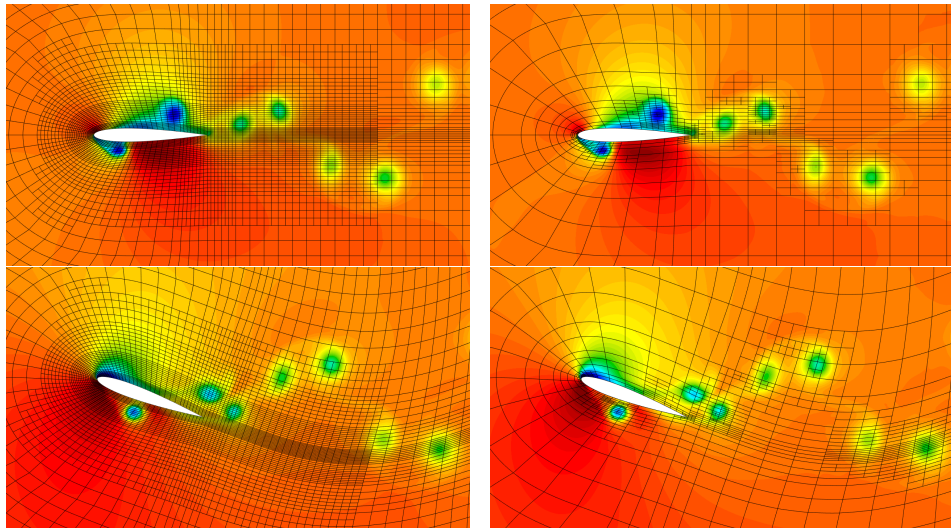


# Laminar Pitching Airfoil

- $M_\infty = 0.2$ ,  $Re = 1000$
- $\Delta\alpha = 20^\circ$ ,  $k = 0.25$
- Separated flow with complex wake pattern
- Level 0 mesh (right): 1248 elements
- 2 level adaptation
- Non-adaptive mesh: 5756 elements

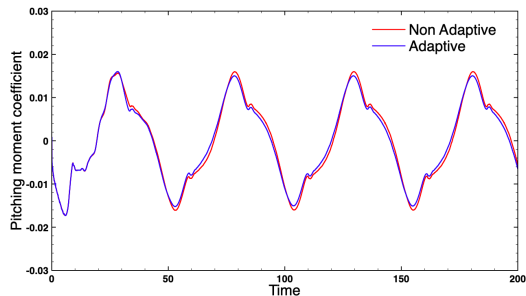
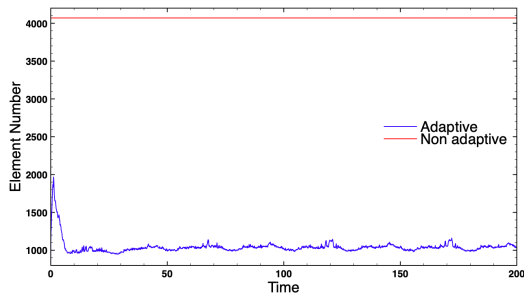
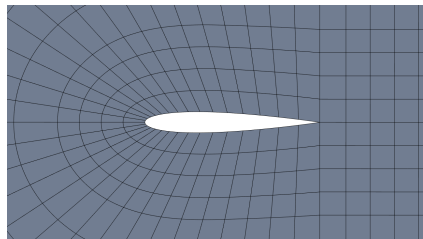


# Laminar Pitching Airfoil



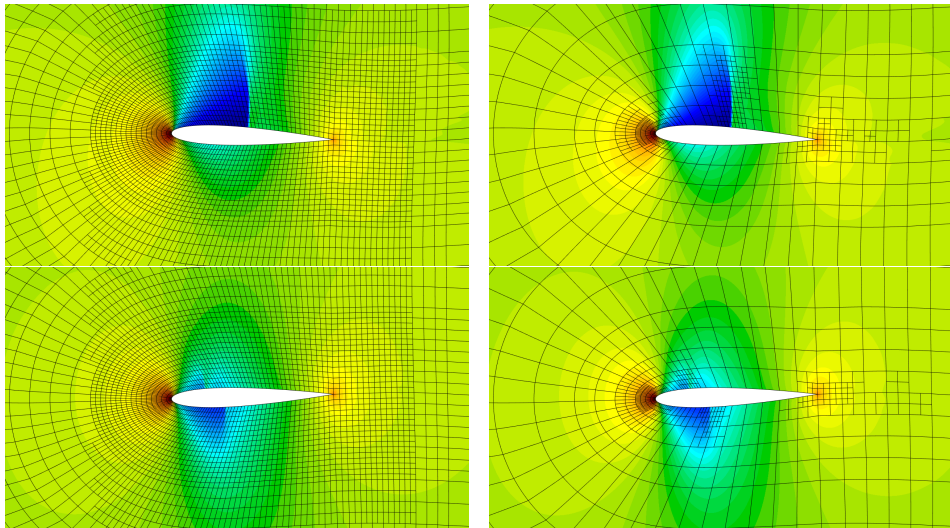
# Transonic Pitching Airfoil

- $M_\infty = 0.755$ , inviscid fluid, with artificial viscosity
- $\alpha_0 = 0.016^\circ$ ,  $\Delta\alpha = 2.51^\circ$ ,  $k = 0.0814$
- Variable intensity moving shock
- Level 0 mesh (right): 720 elements
- 2 level adaptation
- Non-adaptive mesh: 4070 elements





# Transonic Pitching Airfoil



# Conclusions and perspectives

- A DG framework that natively supports CAD geometries
- Curvilinear grids required for a truly high-order scheme
- ALE formulation with NURBS-based grid velocity
- Mesh movement does not impact overall accuracy
- A simple yet effective ALE-AMR coupling algorithm
  
- Further developments:
  - fully conservative sliding meshes
  - fluid-structure interaction
  - shape optimization

**Thanks for your attention!**